ac permeability of defect-free type-II superconductors*

John R. Clem†
Ames Laboratory–ERDA and Department of Physics, Iowa State University, Ames, Iowa 50010

H. R. Kerchner and S. T. Sekula
Solid State Division, Oak Ridge National Laboratory,‡ Oak Ridge, Tennessee 37830

(Received 14 July 1975; revised manuscript received 18 May 1976)

A theoretical and experimental study is presented of ac losses in the mixed state of type-II superconductors when viscous damping dominates flux line motion. The theory describes the ac response of a cylindrical superconductor in the mixed state in a dc magnetic field H and a superposed parallel ac field of arbitrary frequency. The complex ac permeability is found to be related to the flux-flow resistivity $\rho_f(B)$, the differential permeability $\mu'(B) = dB/dH$, the frequency, and the sample radius. Measurements were made of the ac permeability in the frequency range 45–1000 Hz of two NbTa alloys which were prepared to minimize bulk-pinning and surface losses. Values of $\rho_f(B)$ and $\mu'(B)$ derived from the measurements agree qualitatively with the model, but $\rho_f(B)$ shows a weak frequency dependence that may arise from the presence of remnant nonviscous losses.

I. INTRODUCTION

The flux-flow resistivity of superconductors in the mixed state has been a subject of continued experimental and theoretical interest[1,2] since the early work of Kim and co-workers. Experimental measurements have been carried out by passing a current through a sample and measuring the voltage drop across it or by measuring the microwave surface impedance. Measurement of the ac susceptibility has been used for some time as a contactless method of determining resistivity in normal metals.[3] However, measurements of the ac susceptibility or permeability of superconductors have been used only to investigate flux pinning because flux-pinning effects ordinarily dominate the response of superconductors to a low-frequency ac magnetic field.[4,5] By carefully annealing our samples and thermally oxidizing their surfaces, we have been able to reduce flux pinning sufficiently so that viscous damping dominates flux-line motion and ac response.

In this article we discuss the electrodynamics of an infinite cylinder of a superconductor in the mixed state in a large axial dc magnetic field and a parallel small-amplitude ac field. The only limitations on the frequency are that it must be low enough so that displacement-current and energy-gap effects can be neglected. The response of a superconductor to an ac magnetic field arises from the motion of flux lines and can be quantitatively studied by measurements of the complex ac magnetic permeability. This ac response is dependent on the combined influence of bulk and surface pinning of fluxoids as well as viscous drag effects. Solutions to the general problem are extremely difficult to obtain; but in the case of an ideal defect-free type-II superconductor (i.e., in the absence of bulk and surface pinning), the equations can be linearized and a solution obtained for a sufficiently low-amplitude ac field. The solution relates the complex ac permeability $\mu = \mu' + i\mu''$ to the flux-flow resistivity ρ_f, the static differential magnetic permeability $\mu'(B) = dB/dH$, the frequency ω, and the sample radius a.

We report here measurements of the ac permeability of two nearly ideal NbTa alloys as a function of dc magnetic field, frequency, and ac field amplitude at 4.2 K. We find that reasonable values of dB/dH and ρ_f can be deduced from the complex permeability throughout the mixed-state region except for applied fields close to H_{c1}, where the experimental conditions do not satisfy the requirements of the analysis. The values of ρ_f and dB/dH derived from these measurements agree qualitatively with the expected results, but ρ_f shows a weak frequency dependence that may reflect the approximate nature of our simple phenomenological model.

II. THEORY

A. General remarks

The ac magnetic permeability of type-II superconductors is associated with the energy dissipation produced by the motion of quantized vortex lines. Such dissipation can be thought of as arising from local Joule heating in the vortex core, where the time-varying local flux density produces a local electric field, which in turn drives local normal currents through the core. The rate of energy dissipation per unit length of vortex can be written as[1,6] $\eta v_\perp^2$, which can be interpreted as the rate at which work is done by the viscous drag

force per unit length of vortex line, $-\eta\vec{v}_{\parallel}$, where η is called the viscous drag coefficient and $\vec{v}_{\parallel}$ is the component of the vortex line velocity parallel to the local driving force. When the driving forces on a vortex array are generated by the time-dependent component of an applied magnetic field, varying sinusoidally with angular frequency ω, the velocity $\vec{v}_{\parallel}$, in the absence of flux pinning, is proportional to ω, and the total energy dissipation per cycle is frequency dependent, as in the case of eddy-current losses in normal conductors. On the other hand, whenever flux motion is dominated by flux pinning in the superconductor, either in the bulk or at the surface, a vortex, during its trajectory through the specimen, moves with a highly irregular velocity and, in particular, moves very rapidly and irreversibly in the vicinity of pinning sites. According to the theory of dynamic pinning,[7,8] the vortex then dissipates an essentially fixed amount of energy each time it travels past a pinning site. The total energy dissipation per cycle in such a case may be shown to be independent of frequency.

The details of the low-frequency ac magnetic permeability of type-II superconductors are determined by the relative contributions of three possible modes of energy dissipation: viscous losses, bulk-pinning losses, and surface losses. By *viscous losses* we refer to the dissipation that would occur even in the absence of flux pinning; such losses are analogous to eddy-current losses in normal conductors. By *bulk-pinning losses* we refer to dissipation at bulk-pinning sites distributed throughout the specimen interior; such losses are describable in terms of the critical-state model.[4,9] By *surface losses* we refer to the dissipation occurring at the specimen surface: below H_{c2}, via surface-pinning sites[10] or a surface barrier,[11,12] and between H_{c2} and H_{c3}, via the superconducting surface sheath.[13]

Although the low-frequency ac magnetic permeability of heavily pinned hard superconductors is usually dominated by bulk-pinning losses and surface-pinning losses, viscous losses can play an important role in weakly pinned type-II superconductors, especially when the skin depth is roughly of the order of the specimen radius. For the specimens described later in this paper, we believe that viscous losses in fact play the dominant role. Consequently, we shall next summarize the electrodynamic description of type-II superconductors at low frequencies for ideal specimens in which bulk and surface pinning are negligible. This formalism will then be used to calculate the ac magnetic permeability for cylindrical ideal type-II superconductors. At the end of this section, we discuss the possible effects of bulk and surface pinning on measurements of the ac permeability, and we describe several tests that can be experimentally performed to test the validity of neglecting pinning.

B. ac magnetic permeability of an ideal type-II superconducting cylinder

Let us consider an isotropic ideal type-II superconducting specimen of dimensions large by comparison with the penetration depth λ. We consider its isothermal response to electromagnetic disturbances of sufficiently low frequency that the displacement current can be neglected. Let us assume that the specimen contains an inhomogeneously distributed array of interacting quantized vortices (or fluxoids or fluxons), but that the inhomogeneities, or electromagnetic disturbances, vary spatially on a scale of length much larger than the intervortex spacing. These assumptions permit us to average the magnetic flux density over many vortices, and to apply thermodynamic arguments.

In this situation, the *free energy density* F_m of the vortex array can be expressed as a scalar function of B ($B = |\vec{B}|$) and thus varies on the same length scale as B. Since we are considering only isothermal processes, we suppress the dependence of F_m upon the absolute temperature T. The *magnetic field* $\vec{H}$ is obtained from F_m via[14]

$$\vec{H} = 4\pi \frac{\partial F_m(B)}{\partial \vec{B}}. \tag{1}$$

We define a current density $\vec{J}$ via

$$\nabla \times \vec{H} = (4\pi/c)\vec{J}. \tag{2}$$

London[15] called this the "coarse-grained current density," and Campbell and Evetts[16] call it the "transport current density." From a thermodynamic analysis, one may show that when $\vec{B}$ varies spatially such that $\vec{J}$ does not vanish, the vortex array is not in over-all thermodynamic equilibrium and will move with velocity $\vec{v}$ (perpendicular to $\vec{B}$) in such a way as to minimize the free energy. The corresponding force per unit volume driving the vortex array towards equilibrium is then[17]

$$\vec{F} = \vec{J} \times \vec{B}/c. \tag{3}$$

As a result of the motion, an electric field

$$\vec{E} = \vec{B} \times \vec{v}/c \tag{4}$$

is generated, which varies on the same length scale as B and v.

In the absence of flux pinning, the flux-flow velocity $\vec{v}$ and the electric field $\vec{E}$ are determined by a balance between the viscous drag force $\eta\vec{v}$

and the force $\vec{F}$. Then $\vec{E}$ is proportional to $\vec{J}$. Introducing the flux-flow resistivity[2] ρ_f, which depends upon B and T, we can write

$$\vec{E} = \rho_f \vec{J}. \tag{5}$$

Since the materials discussed in this paper are alloys, in which the electron mean free path is much smaller than the cyclotron radius at H_{c2}, we neglect the Hall field.

We now specialize to the case of an infinite ideal type-II superconducting cylinder of radius a in the presence of a longitudinal time-dependent applied field $\vec{H}_a(t)$. It is convenient to regard the cylinder as centered on the z axis and to use cylindrical coordinates $\rho = (x^2+y^2)^{1/2}$, $\phi = \tan^{-1}(y/x)$, and z with unit vectors $\hat{\rho} = \hat{x}\cos\phi + \hat{y}\sin\phi$, $\hat{\phi} = \hat{y}\cos\phi - \hat{x}\sin\phi$, and $\hat{z}$, such that $\vec{H}_a = H_a\hat{z}$. We assume that $\vec{B}$, $\vec{H}$, $\vec{J}$, $\vec{v}$, and $\vec{E}$ depend only upon ρ. Then we obtain $\vec{B} = B_z\hat{z}$, $\vec{H} = H_z\hat{z}$, and $\vec{J} = J_\phi\hat{\phi}$, where, from Eq. (2), we obtain

$$-\frac{\partial H_z}{\partial \rho} = \frac{4\pi}{c} J_\phi. \tag{6}$$

From Eqs. (4) and (5) we obtain $\vec{E} = E_\phi\hat{\phi}$, where

$$E_\phi = \rho_f J_\phi. \tag{7}$$

Faraday's law becomes

$$\rho^{-1}\frac{\partial(\rho E_\phi)}{\partial \rho} + c^{-1}\frac{\partial B_z}{\partial t} = 0. \tag{8}$$

The above equations, subject to the boundary conditions $H_z(a, t) = H_a(t)$, describe a well-defined problem in electrodynamics. If H_a makes large excursions that are appreciable fractions of the fields H_{c1} and H_{c2} characteristic of the superconductor, the solution is very difficult to obtain, because the B dependence of H and ρ_f makes the field equations nonlinear. However, if

$$H_a(t) = H_0 + h_0\cos\omega t, \tag{9}$$

where $h_0 \ll H_0$, the above equations can be linearized and a solution easily obtained.

If $h_0 = 0$, the steady-state solutions in the superconductor are $H_z = H_0$, $B_z = B_0 = B_{eq}(H_0)$, where $B_{eq}(H)$ is the equilibrium value of B for a given value of $H = 4\pi\partial F_m/\partial B$ inside the superconductor, and $\vec{E} = \vec{J} = 0$. We denote these as zero-order solutions.

If $0 < h_0 \ll H_0$, all quantities may be expanded in powers of h_0/H_0. Retaining only the zero- and first-order terms, we obtain

$$H_z = H_0 + H_1, \tag{10}$$

$$B_z = B_0 + B_1, \tag{11}$$

$$J_\phi = J_1, \tag{12}$$

$$\vec{E} = \vec{E}_1 = E_{1\phi}\hat{\phi}, \tag{13}$$

where the quantities with the subscript "1" are dependent upon ρ and t and are proportional to h_0. Substituting these quantities into Eqs. (6)–(8), expanding all quantities in powers of h_0, and retaining only first-order terms, we obtain

$$-\frac{\partial H_1}{\partial \rho} = \frac{4\pi}{c} J_1, \tag{14}$$

$$E_{1\phi} = \rho_{f0} J_1, \tag{15}$$

$$\rho^{-1}\frac{\partial(\rho E_{1\phi})}{\partial \rho} + \frac{\mu_0'}{c}\frac{\partial H_1}{\partial t} = 0, \tag{16}$$

where $\rho_{f0} = \rho_f(B_0)$, and

$$\mu_0' = \mu'(B_0) = \frac{dB_{eq}(H_0)}{dH_0} = \left(\frac{dH_{eq}(B_0)}{dB_0}\right)^{-1}. \tag{17}$$

Combining Eqs. (14)–(16), we obtain as the fundamental equation in the superconductor

$$\frac{\partial H_1}{\partial t} = D_{f0}\rho^{-1}\frac{\partial(\rho\partial H_1/\partial\rho)}{\partial \rho}, \tag{18}$$

which is a diffusion equation for perturbations of the magnetic field H and is to be solved subject to the boundary condition that $H_1(a, t) = h_0\cos\omega t$. The diffusion is governed by the flux-flow magnetic diffusivity

$$D_{f0} = D_f(B_0) = c^2\rho_{f0}/4\pi\mu_0', \tag{19}$$

which depends strongly upon the magnetic flux density B_0. For small B_0, where $\rho_{f0} \ll \rho_n$ and $\mu_0' \gg 1$, we obtain $D_{f0} \ll D_n$, where D_n is the normal-state magnetic diffusivity

$$D_n = c^2\rho_n/4\pi. \tag{20}$$

D_{f0} increases with increasing B_0 up to the value

$$D_f(H_{c2}) = c^2\rho_n/4\pi\mu'(H_{c2}), \tag{21}$$

where $\rho_f(H_{c2}) = \rho_n$ and $\mu'(H_{c2}) > 1$. The magnetic diffusivity has a discontinuity at $B_0 = H_{c2}$, since $D_f(H_{c2})$ is smaller than the value D_n in the normal state just above H_{c2}.

Equation (18) is easily solved by writing the sinusoidally varying part of the applied field as $\mathrm{Re}h_0e^{-i\omega t}$ and by writing $H_1(\rho, t) = \mathrm{Re}h_1e^{-i\omega t}$, where Re denotes the real part, and $h_1(\rho)$, a complex quantity, obeys the boundary condition $h_1(a) = h_0$. Equation (18) then becomes

$$-i\omega h_1 = D_{f0}\rho^{-1}\frac{d(\rho dh_1/d\rho)}{d\rho}, \tag{22}$$

which is Bessel's equation of order zero with the solution

$$h_1(\rho) = h_0 J_0(k\rho)/J_0(ka). \tag{23}$$

Here, J_0 is the Bessel function of order zero, $k = (1+i)/\delta_{f0}$, and δ_{f0} is the *flux-flow skin depth*, defined by

$$\delta_{f0}^2 = 2D_{f0}/\omega = c^2\rho_{f0}/2\pi\omega\mu_0'. \quad (24)$$

Note that as B_0 increases from zero to H_{c2}, δ_{f0} increases from zero to a value a little less than the normal-state skin depth, defined by

$$\delta_n^2 = 2D_n/\omega = c^2\rho_n/2\pi\omega. \quad (25)$$

Thus, the first-order time-dependent flux density is

$$B_1(\rho, t) = \mu_0' \mathrm{Re}[h_0 e^{-i\omega t} J_0(k\rho)/J_0(ka)] \quad (26)$$

and the average flux density contained in the cylinder is

$$\overline{B}_1(t) = \frac{2}{a^2}\int_0^a d\rho\, \rho B_1(\rho, t)$$
$$= \mu_0' \mathrm{Re}[h_0 e^{-i\omega t} 2J_1(ka)/(ka)J_0(ka)]. \quad (27)$$

The complex permeability $\mu = \mu' + i\mu''$ is defined via

$$\overline{B}_1(t) = \mathrm{Re}(\mu h_0 e^{-i\omega t})$$
$$= \mu' h_0 \cos\omega t + \mu'' h_0 \sin\omega t, \quad (28)$$

such that

$$\mu/\mu_0' = 2J_1(ka)/(ka)J_0(ka). \quad (29)$$

The result also may be expressed in terms of the modulus M_ν and phase θ_ν of the Kelvin functions[18]:

$$\mu/\mu_0' = f_0 e^{i\beta}, \quad (30)$$

where

$$f_0(x) = 2M_1(x)/xM_0(x), \quad (31)$$

$$\beta(x) = \theta_0(x) - \theta_1(x) + \tfrac{3}{4}\pi, \quad (32)$$

$$x = a\sqrt{2}/\delta_{f0}. \quad (33)$$

Thus,

$$\mu'/\mu_0' = f_1 = f_0 \cos\beta, \quad (34)$$

$$\mu''/\mu_0' = f_2 = f_0 \sin\beta, \quad (35)$$

and

$$\mu''/\mu' = \tan\beta. \quad (36)$$

Plots of f_0, f_1, f_2, and $\tan\beta$ are shown in Fig. 1.

The form of Eqs. (30)–(36) suggests a method for determining the values of μ_0' and ρ_{f0} from experimental values of μ' and μ'', provided the angular frequency ω and the specimen radius a are known. By inverting Eq. (36), the appropriate value of x can be obtained. Since f_0, f_1, f_2, and β then are known, μ_0' can be obtained from Eq. (34) or (35). Finally, ρ_{f0} can be obtained from Eqs. (24) and (33). We expect the precision of the method to be optimized when μ''/μ_0' is close to its maximum value near $x = 2.5$, which occurs when the flux-flow skin depth δ_f is roughly equal to the specimen radius a. This method is closely related to that proposed by Chambers and Park[3] for the determination of the normal-state resistivity. Our results, in fact, reduce to theirs if we make the replacements $\mu_0' \to 1$, $\rho_{f0} \to \rho_n$, and $\delta_{f0} \to \delta_n$.

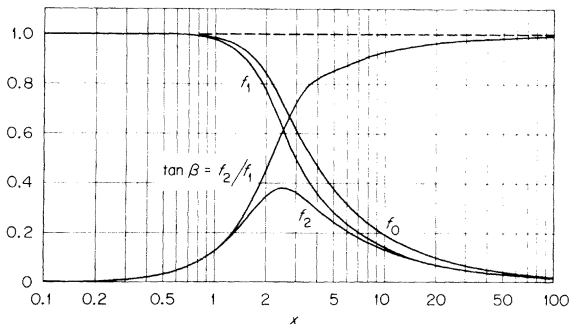

FIG. 1. Auxiliary functions used in the analysis, f_0, f_1, f_2, and $\tan\beta = f_2/f_1$, defined by Eqs. (30)–(36), vs $x = a\sqrt{2}/\delta_{f0}$, where a is the specimen radius and δ_{f0} is the flux-flow skin depth.

C. Limits of applicability of the model

The ac magnetic permeability of a long type-II superconducting cylinder is dependent not only on viscous losses but can be influenced by bulk and surface pinning. As mentioned in Sec. II A, the loss per cycle due to pinning is independent of frequency and in addition depends on ac field amplitude h_0 in a nonlinear way.[4,9-13] In order to minimize the effects of pinning, the ac field amplitude should be sufficiently large that the induced current density greatly exceeds the pinning critical current density over most of the sample during a large portion of the cycle. On the other hand, the method we propose to interpret the data requires a small ac field amplitude. Our proposed method probes $\mu'(B) = dB/dH$ and $\rho_f(B)$ over a range of flux densities centered on $B = B_0$ with a resolution width $2\mu_0' h_0$. Structure in $\mu'(B)$ and $\rho_f(B)$ can be resolved only if its width is larger than the resolution width. Furthermore, if the ac field amplitude is too large, structure in $\mu'(B)$ and $\rho_f(B)$ may give rise to nonlinear response and an amplitude-dependent ac permeability. To determine whether our proposed method is working properly in a given experimental situation and whether our basic assumptions, that viscous damping is dominant and that the ac field amplitude is small compared to structure in $\mu'(B)$ and $\rho_f(B)$, are correct, the following experimental tests can be made.

1. Dependence upon amplitude h_0. As discussed above, if the method is working properly, there should be no dependence of μ' and μ'' upon the amplitude h_0. An amplitude dependence indicates either structure in μ_0' and ρ_{f0} at the limits of reso-

lution or contributions from bulk and surface pinning.

2. *Dependence upon H_0 above H_{c2}.* If surface pinning is negligible, there should be no dependence of μ' and μ'' upon H_0 above H_{c2}. An H_0 dependence indicates surface losses, which probably persist and are even larger below H_{c2}.

3. *Dependence upon ω.* If surface and bulk pinning are negligible, there should be a strong dependence of μ' and μ'' upon ω through the frequency dependence of the flux-flow skin depth δ_{f0}. Furthermore, the values of μ_0' and ρ_{f0}, calculated using the proposed method, should be frequency independent. Surface- and bulk-pinning contributions to μ' and μ'' introduce apparent errors, which propagate into the calculated values of x, μ_0', and ρ_{f0}, leading to a spurious frequency dependence of both μ_0' and ρ_{f0}. If surface- and bulk-pinning losses greatly exceed viscous damping losses, as is the case for very low frequency ω, the resulting experimental values of $\mu'$and μ'' are frequency independent.

4. *Dependence upon magnetic history.* If surface and bulk pinning are negligible, there should be no dependence of μ' and μ'' upon the history of H_0, since flux is then swept in and out of the specimen over its entire cross section during each cycle. Differences in μ' and μ'' observed in increasing and decreasing fields H_0 indicate trapped flux, which is *not* swept in and out during each cycle. The existence of this trapped flux implies that surface- and bulk-pinning contributions to μ' and μ'' are not negligible. With hysteresis, there is a smaller amount of flux threading the middle of the specimen in a given applied field H_0 when the field was increased to that value than when it was decreased. Those segments of the trapped vortices that are pinned near the center of the specimen dissipate no energy and thus make no contribution to μ'' or μ'. However, since the remaining segments of these vortices *do* move in response to the strong currents that flow where the vortices intersect the specimen surface, they dissipate energy and therefore contribute to μ'' and μ'. The difference in the density of these moving segments in the field-increasing and field-decreasing cases thus accounts for the differences in μ'' and μ' in the two cases.

III. EXPERIMENT

A. Sample preparation

The NbTa alloys were prepared from Nb and Ta powders by arc melting on a water-cooled copper hearth. The molten metals were then drop cast into rods approximately 1 cm in diameter. A rod of each alloy was swaged to 3.2 mm diameter, double-pass zone refined, and then spark machined to a prolate spheroid. Each sample was chemically polished and annealed for 5 h at 2360°C in a vacuum of 5×10^{-9} Torr. Finally, the samples were heated to 400°C for 2 min in 1 atm of pure oxygen. This last step has been shown to reduce the magnetic hysteresis of single-crystal niobium samples without altering the purity or crystalline structure of the bulk of the sample.[19,20]

We determined the composition of the samples by chemical analysis of adjacent sections of the rod from which each sample was machined. The dimensions of the samples are given in Table I.

B. Measurement technique

We measured the ac permeability by using a Hartshorn mutual-inductance bridge that was previously used in this laboratory for measuring critical current densities.[5] We balanced the bridge with the sample in place in zero dc applied field. In this situation (i.e., the Meissner state), the ac field is excluded from the interior of the sample so that the permeability is zero. Then, when the ac permeability is nonzero, the signal across the secondary of the bridge is proportional to the time derivative of the average magnetic induction in the sample. A lock-in amplifier with a two-phase accessory produced dc output voltages in proportion to the real and imaginary parts of the ac permeability, μ' and μ''. The phase setting of the lock-in and the output voltage corresponding to a permeability of unity were determined by removing the sample from the secondary of the bridge.

For each measurement, we ramped the dc field

TABLE I. Characteristics of the two samples discussed in the text.

	Sample 1	Sample 2
Composition (at.% tantalum)	0.5%	11%
Major diameter (cm)	2.5	2.5
Minor diameter (cm)	0.27	0.27
Demagnetization factor	0.025	0.025
H_{c2} at 4.2 K (kOe)	2.87	4.42
ρ_n ($\mu\Omega$ cm)	0.115	1.83
x_n (45 Hz)	0.699	
x_n (88 Hz)	0.977	
x_n (350 Hz)	1.949	0.489
x_n (1000 Hz)		0.826

at a constant rate (5.3 Oe/sec for sample 1 and 7.6 Oe/sec for sample 2) from zero field to above H_{c2} and then back to zero. We graphed the output voltages proportional to μ' and μ'' versus the current through the dc-field coil directly by using a two-pen X-Y recorder. To facilitate subsequent data analysis, these three quantities were also recorded digitally on paper tape at 10-sec intervals. In order to obtain reliable values for the normal-state resistivity, we measured the ac permeability at the highest field attainable with our dc magnet, about 10 kOe. This field was about $2H_{c2}$ for sample 2 and $3.5H_{c2}$ for sample 1.

C. Results

The surface oxidation treatment substantially reduced the hysteresis in the dc magnetization curves, as shown in Fig. 2. In addition, the results of our ac permeability measurements pass the tests discussed in Sec. IIC quite well, indicating the dominance of viscous damping. Some discrepancies, however, suggest that remnant nonviscous losses may be influencing our measurements. In Sec. IV, we discuss the degree to which our experimental results satisfy the requirements of the four tests mentioned previously.

We measured μ' and μ'' as functions of the applied dc field H_0, the amplitude h_0 of the applied ac field, and the frequency ω. In order to use the theory described in Sec. II, it was necessary to

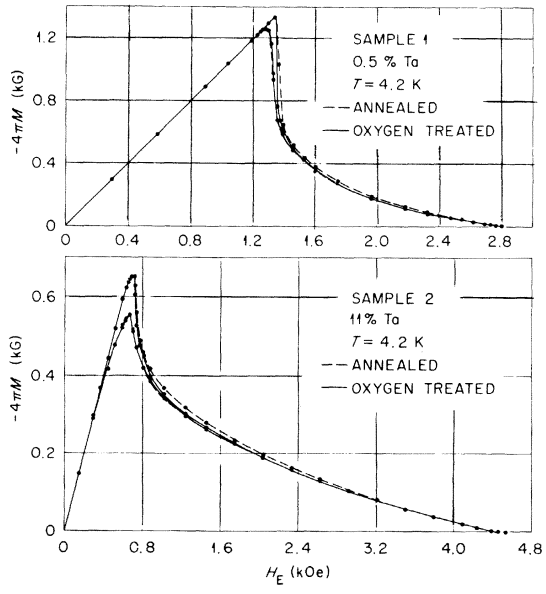

FIG. 2. Measurements of the dc magnetization before and after the thermal oxidation treatment. The magnetization is plotted vs the effective field $H_E = H_0 - 4\pi M\eta$, where $\eta = 0.025$ for these samples.

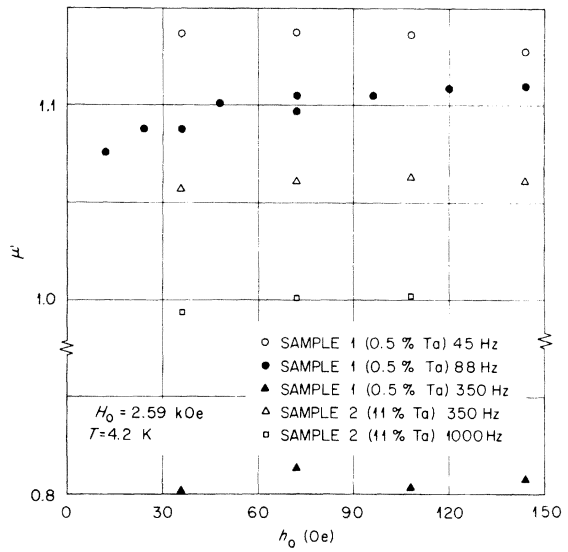

FIG. 3. Measurements of the real part of the ac permeability μ' plotted vs the amplitude of the applied ac field.

assume that our prolate spheroids approximated infinite cylinders. The value for the sample radius used in the analysis was deduced by comparing the $\mu' = 1$ signals for the prolate spheroids with those of a superconducting cylinder of similar dimensions. This value was 8% smaller than the minor radius of the prolate spheroids.

The values of ρ_n given in Table I are averages of values obtained from measurements of μ' and

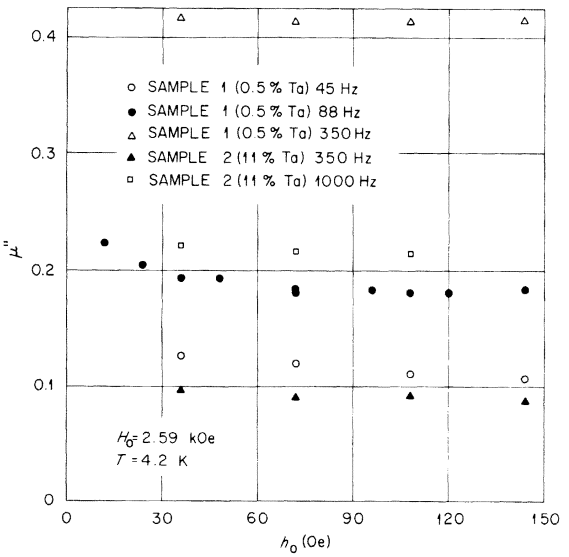

FIG. 4. Measurements of the imaginary part of the ac permeability μ'' plotted vs the amplitude of the applied ac field.

μ'' at 10 kOe and at several frequencies and amplitudes. The scatter of the individual determinations of ρ_n appears to be random and shows an rms deviation of 2%. The values of μ_0' that we derived from the measurements at 10 kOe are all within 0.5% of unity.

In Figs. 3 and 4 are shown values of μ' and μ'' plotted against the ac field amplitude h_0 for both samples in the mixed state. Both components of the ac permeability are amplitude dependent at low amplitudes, but are nearly constant for h_0 greater than about 50 Oe. As one would expect, the largest amplitude dependence is associated with the lowest frequency (45 Hz), which gives the smallest values of μ''/μ_0'.

Our measurements of μ' and μ'' are graphed as functions of H_0 in Figs. 5 and 6. Both components of the permeability depend strongly on the frequency at all fields ($H_0 > H_{c1}$) and on the applied field in the mixed-state region ($H_{c1} < H_0 < H_{c2}$). The differential paramagnetic effect ($\mu_0' > 1$) is clearly evident in the lower-frequency μ' curves. The discontinuity in μ_0' at H_{c2} shows up clearly in all the curves. Also shown in these figures is the value of $2h_0/H_{c2}$, the reduced field resolution width. Note that details in μ' and μ'' vs H_0 near H_{c1} and H_{c2} are smeared out over this width. The curves shown were measured in increasing field. No hysteresis was observable, except for H_0 between $H_{c1} - h_0$ and $H_{c1} + h_0$.

Our results for ρ_{f0} and μ_0' are plotted in Figs. 7 and 8 as functions of the dc magnetic induction B_0. The value of $2h_0/H_{c2}$ shown in these figures

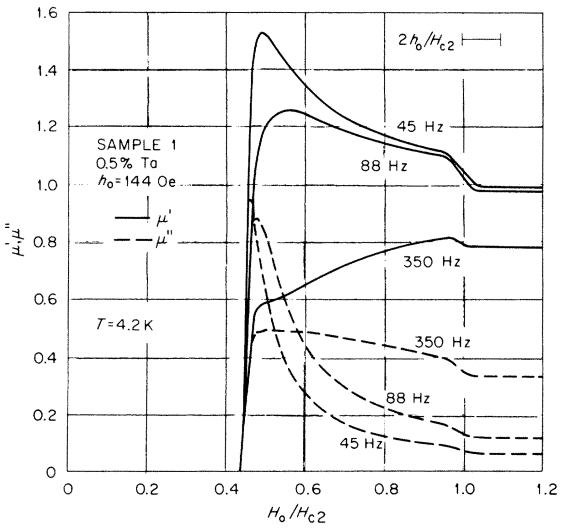

FIG. 5. Measurements of the real and imaginary parts of the ac permeability plotted as a function of dc applied field H_0 for sample 1.

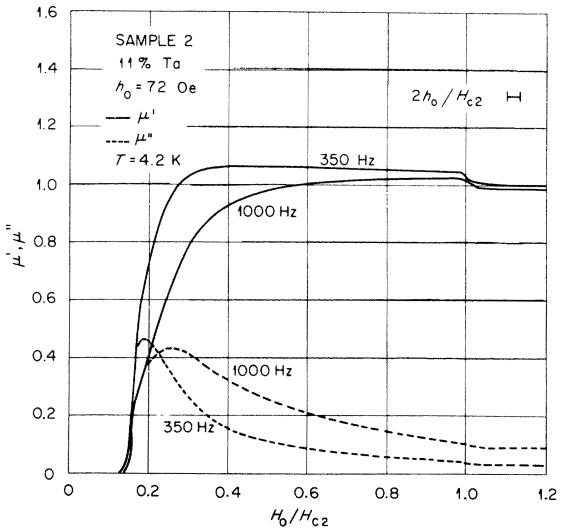

FIG. 6. Measurements of the real and imaginary parts of the ac permeability plotted as a function of dc applied field H_0 for sample 2.

is an approximate measure of the resolution; the reduced flux density resolution width is actually $2\mu_0' h_0/H_{c2}$, which depends upon B_0. The flux-flow resistivity is normalized by the (average) normal-state resistivity of Table I, and B_0 is normalized by the upper critical field H_{c2}.

For comparison, we also have plotted in Figs. 7 and 8 μ_0' as derived from the dc magnetization measurements and the empirical rule, ρ_{f0}/ρ_n

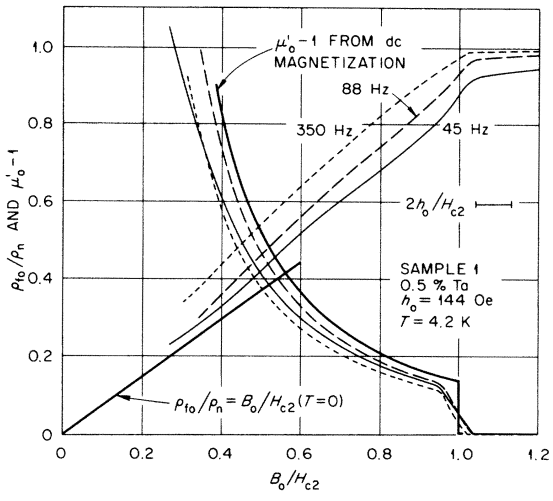

FIG. 7. Flux-flow resistivity ρ_{f0}, normalized to the normal-state value ρ_n, and the differential permeability μ_0' derived from the ac permeability measurements, plotted as a function of the dc magnetic induction B_0, for sample 1. Included for comparison are plots of μ_0' derived from the dc magnetization measurements and of the empirical rule for ρ_{f0}/ρ_n from Ref. 1.

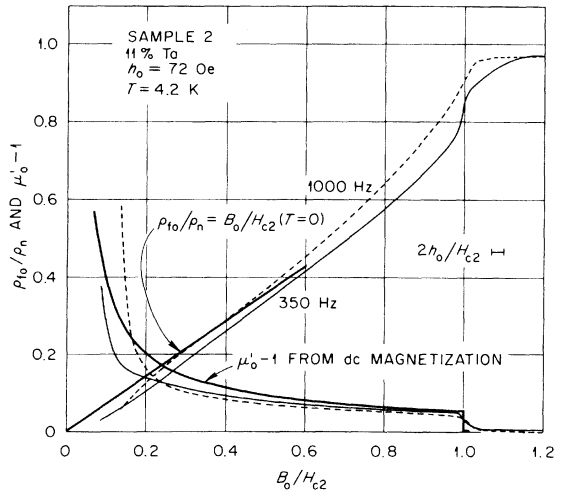

FIG. 8. Flux-flow resistivity ρ_{f0}, normalized to the normal-state value ρ_n, and the differential permeability μ_0', derived from the ac permeability measurements, plotted as a function of the dc magnetic induction B_0, for sample 2. Included for comparison are plots of μ_0' derived from the dc magnetization measurements and of the empirical rule for ρ_{f0}/ρ_n from Ref. 1.

$= B_0/H_{c2}(T=0)$, deduced by Kim, Hempstead, and Strnad, from their dc flux-flow–resistivity measurements.[1] It should be pointed out that the data presented in Ref. 1 for intermediate temperatures (near our temperature of 4.2 K) obey the empirical rule accurately only for B_0 less than approximately $0.6H_{c2}$. For larger B_0, Kim *et al.* and other investigators have found $\rho_{f0}/\rho_n > B_0/H_{c2}(T=0)$.

In order to interpolate the dc magnetization data to obtain B as a function of H and μ_0' as a function of B, we fitted an expression of the form suggested by Kes *et al.*[21] to the experimental data. This expression fit the data to within 0.1% H_{c2} for H greater than $1.3H_{c1}$. In these calculations, we took account of the demagnetization coefficients of each sample.

IV. CONCLUSIONS

A. Tests for applicability of the model

In this section we apply the tests of Sec. II C to our experimental results in order to determine the applicability of the theoretical model.

1. Dependence upon amplitude h_0. The data presented in Figs. 3 and 4 indicate that, while some residual pinning of flux lines remains in these samples, it is possible to apply a sufficiently high amplitude ac field that amplitude dependence becomes negligible and still have good experimental resolution. Additional data (not presented here) taken over the whole range of applied fields, $H_{c1} + h_0 < H_0 < 1.2H_{c2}$, show the same qualitative behavior as shown in Figs. 3 and 4.

2. Dependence upon H_0 above H_{c2}. Both μ' and μ'' depend slightly upon the applied field in the range $H_{c2} + h_0 < H_0 < 1.2H_{c2}$, although this is not apparent from Figs. 5 and 6. The resulting resistivities for these fields lie slightly below the normal-state resistivity (measured at $H_0 = 10$ kOe). (See Figs. 7 and 8.) As was found for the amplitude dependence, the largest deviation from the ideal behavior occurs for the 45-Hz data. Resistivities measured at the higher frequencies at $1.2H_{c2}$ lie within 2% of the true normal-state resistivities. We conclude that a surface barrier or surface pinning is present; its influence upon the results is small above H_{c2}, except at 45 Hz, but unknown below H_{c2}.

3. Dependence upon ω. As expected, μ' and μ'' (Figs. 4 and 5) show a strong frequency dependence, which is indicative of viscous drag effects. However, the flux-flow resistivities that we deduce show a weak frequency dependence. Moreover, the over-all shape of the resistivity curves of Figs. 7 and 8 deviate significantly from previous data.[1,2] Although the lowest-frequency curve for each sample most closely matches previous results, it is the lowest-frequency data that flux pinning appears to influence most.

4. Dependence upon magnetic history. As noted above, except for applied fields H_0 within h_0 of H_{c1} there was no observable hysteresis in the measured values of μ' and μ''. The limit of resolution of this observation is the hysteresis, about 10 Oe, of our superconducting dc magnet.

B. End effects

Since our samples are not truly long compared with the dimensions of our pickup coil (in fact, they are of comparable size), end effects may introduce systematic errors. One can easily show, for example, that the normal-state resistivity obtained from measurements on a spherical sample and the equations for an infinite cylinder would show a spurious dependence in the same direction as the frequency dependence we found.

We performed three experimental tests to determine the importance of end effects to our measurements. From the results of these tests, we conclude that end effects cannot account for the observed frequency dependence of ρ_f. First, if end effects were responsible for the apparent frequency dependence in ρ_{f0}, one would expect ρ_n to be frequency dependent (but probably less so because end effects should be most important when x is large). We could observe no systematic frequency dependence in ρ_n. A second test of the sig-

nificance of end effects is to measure the effect on μ_n', μ_n'', and ρ_n of moving the sample with respect to the pickup coil. Moving sample 1 ($x_n = 1.94$ at 350 Hz) by 3 mm changed μ_n', μ_n'', and ρ_n by less than 1%. Moving a pure niobium sample of similar dimensions ($x_n = 3.12$ at 47 Hz) by 3 mm changed μ_n', μ_n'', and ρ_n by less than 1.3%. A third test of the significance of end effects is to repeat the measurements with coils of different sizes. Measurements made with two sets of pickup coils $\frac{1}{2}$ and $\frac{1}{4}$ in. long showed no systematic differences.

C. Summary

We have presented here a theory for the ac permeability of a type-II superconductor whose ac losses are dominated by viscous damping. Qualitatively, the theory describes the ac response of our NbTa samples quite well. However, some quantitative discrepancies remain. The weak field dependence of μ' and μ'' above H_{c2} implies the presence of surface pinning or a surface barrier. The amplitude dependence at small amplitudes in the mixed state also implies the presence of nonviscous losses. Although it would appear that using an ac field of sufficiently high amplitude should make flux-pinning effects negligible, our experimental results for the flux-flow resistivity show significant deviations from those we would expect. We believe the explanation for these deviations is that remnant flux pinning introduces significant errors into the interpretation of our results. Unfortunately, the influence of flux pinning on ac permeability measurements is sufficiently complex that we cannot make quantitative estimates of its importance; therefore, we cannot provide a solid explanation for the deviations observed. We are currently investigating ac response at low frequencies when both flux-pinning and viscous-drag effects are important.

ACKNOWLEDGMENTS

The authors are grateful to R. E. Reed and E. D. Bolling for furnishing the samples and carrying out the annealing procedures. We also wish to thank R. H. Kernohan for making the dc magnetization measurements. One of us (J.R.C.) expresses his appreciation to Professor G. Eilenberger for his hospitality at the Institut für Festkörperforschung of the Kernforschungsanlage Jülich, where some of this work was carried out.

---

*Prepared for the U.S. Energy Research and Development Administration under contracts Nos. W-7405-eng-82 and W-7405-eng-26.

†Supported by a Senior Fulbright-Hays Research Grant.

‡Operated by Union Carbide Corporation for ERDA.

[1]Y. B. Kim, C. F. Hempstead, and A. R. Strnad, Phys. Rev. 139, A1163 (1965).

[2]For a good review of flux flow, see Y. B. Kim and M. J. Stephen, in *Superconductivity*, edited by R. D. Parks (Marcel Dekker, New York, 1969), Vol. 2, Chap. 19, pp. 1107–1165.

[3]R. G. Chambers and J. G. Park, Br. J. Appl. Phys. 12, 507 (1961).

[4]C. P. Bean, Rev. Mod. Phys. 36, 31 (1964).

[5]S. T. Sekula, J. Appl. Phys. 42, 16 (1971).

[6]J. Bardeen and M. J. Stephen, Phys. Rev. 140, A1197 (1965).

[7]K. Yamafuji and F. Irie, Phys. Lett. A 25, 387 (1967).

[8]J. Lowell, J. Phys. C 3, 712 (1970).

[9]For a good review of the critical state model, see A. M. Campbell and J. E. Evetts, *Critical Currents in Superconductors* (Taylor and Francis, London, 1972), p. 45.

[10]E. J. Kramer and A. Das Gupta, Philos. Mag. 26, 769 (1972).

[11]H. A. Ullmaier, Phys. Status Solidi 17, 631 (1966).

[12]S. T. Sekula and J. H. Barrett, Appl. Phys. Lett. 17, 204 (1970).

[13]R. W. Rollins and J. Silcox, Phys. Rev. 155, 404 (1967).

[14]For a more detailed discussion, see Ref. 9, p. 14.

[15]F. London, *Superfluids* (Dover, New York, 1961), Vol. 1, p. 102.

[16]Reference 9, p. 19.

[17]B. D. Josephson, Phys. Rev. 152, 211 (1966).

[18]*Handbook of Mathematical Functions*, edited by M. Abramowitz and I. A. Stegun, U.S. Natl. Bur. Stand. Appl. Math. Series No. 55 (U.S. GPO, Washington, D.C., 1967), p. 382.

[19]H. Berndt, N. Kartascheff, and H. Wenzl, Z. Angew. Phys. 24, 305 (1968).

[20]S. T. Sekula and R. H. Kernohan, Phys. Rev. B 5, 904 (1972).

[21]P. H. Kes, C. A. M. van der Klein, and D. de Klerk, J. Low Temp. Phys. 10, 759 (1973).